CHAOS
Theory and Applications
in Applied Sciences and Engineering

e-ISSN: 2687-4539
RESEARCH ARTICLE
Vol.5 / No.3 / 2023 / pp.198-206
https://doi.org/10.51537/chaos.1321533

A New Fractional-order Derivative-based Nonlinear Anisotropic Diffusion Model for Biomedical Imaging

Alka Chauhan *,1, **Santosh Kumar** *,2 and **Yeliz Karaca** α,3

*Department of Mathematics, Sharda School of Basic Sciences and Research, Sharda University Greater Noida-201310 UP, India, αUniversity of Massachusetts (*UMass*) Chan Medical School, Worcester, MA 01655, USA.

ABSTRACT Medical imaging, the process of visual representation of different organs and tissues of the human body, is employed for monitoring the normal as well as abnormal anatomy and physiology of the body. Imaging which can provide healthcare solutions ensuring a regular measurement of various complex diseases plays a critical role in the diagnosis and management of many complex diseases and medical conditions, and the quality of a medical image, which is not a single factor but a composite of contrast, artifacts, distortion, noise, blur, and so forth, depends on several factors such as the characteristics of the equipment, the imaging method in question as well as the imaging variables chosen by the operator. The medical images (ultrasound image, X-rays, CT scans, MRIs, etc.) may lose significant features and become degraded due to the emergence of noise as a result of which the process of improvement pertaining to medical images has become a thought-provoking area of inquiry with challenges related to detecting the speckle noise in the images and finding the applicable solution in a timely manner. The partial differential equations (PDEs), in this sense, can be used extensively in different aspects with regard to image processing ranging from filtering to restoration, segmentation to edge enhancement and detection, denoising in particular, among the other ones. In this research paper, we present a conformable fractional derivative-based anisotropic diffusion model for removing speckle noise in ultrasound images. The proposed model providing to be efficient in reducing noise by preserving the essential image features like edges, corners and other sharp structures for ultrasound images in comparison to the classical anisotropic diffusion model. Furthermore, we aim at proving the viscosity solution of the fractional diffusion model. The finite difference method is used to discretize the fractional diffusion model and classical diffusion models. The peak signal-to-noise ratio (PSNR) is used for the quality of the smooth images. The comparative experimental results corroborate that the proposed, developed and extended mathematical model is capable of denoising and preserving the significant features in ultrasound towards better accuracy, precision and examination within the framework of biomedical imaging and other related medical, clinical, and image-signal related applied as well as computational processes.

KEYWORDS
Anisotropic diffusion model
Nonlinear mathematical diffusion model
Fractional diffusion model
Fractional order derivatives
Biomedical imaging
Image processing
Denoising
Chaotic signals and noise
Image smoothing
Viscosity solution
Explicit scheme
Multiplicative noise
Conformable fractional derivative
Partial differential equations (PDEs)

INTRODUCTION

Nonlinear anisotropic diffusion equations ensure the enhancement of the image quality through the removal of noise while retaining the subtle details and edges (Gilboa *et al.* 2006). Image denoising is observed to be of utmost importance in image processing as well as in computer vision in order that images can be prepared with better resolutions. Given this, partial differential equations (PDEs) can extensively be employed in different aspects related to image processing ranginging from filtering to restoration, segmentation to edge enhancement and detection, denoising in particular, amongst the other ones (Mazloum and Siahkal-Mahalle 2022). Chaos, as a ubiquitous phenomenon in nature, reveals that the observed chaotic and noisy signals are often disrupted by external interferences. Edge, as one of the most remarkable features for images, requires denoising via nonlinear means and wavelet transform to

Manuscript received: 1 July 2023,
Revised: 27 September 2023,
Accepted: 10 October 2023.

[1]alkachauhan5490@gmail.com
[2]skykumar87@gmail.com
[3]yeliz.karaca@ieee.org (**Corresponding author**).

attain optimal outcomes. When it comes to the image quality, if the additive degrades the quality of the images, it could be possible to end up with diagnostic failures. Ultrasonography, as a biomedical technique, produces the internal structure of the body and gives a great amount of information for clinical diagnosis and treatment. Considering these, detecting the additive noise in the images and finding the solution to such matters becomes a formidable challenge for researchers, clinicians, pharmaceutical authorities and related practitioners.

Speckle noise is the multiplicative noise, and the distorted image is the product of the original image and speckle noise. The Speckle noise can be expressed as:

$$u_0(i,j) = u(i,j) \times S_n(i,j),$$

where $u_0(i,j)$ denotes the noisy image, and let $u(i,j)$ denote the corresponding noiseless image and $S_n(i,j)$ represent the speckle noise.

Manifesting itself in the digital image in a randomly uncorrelated way, noise makes it unavoidable to degrade the visual quality of the images which restricts the accuracy and precision related to interpretation and examination processes. Imaging techniques ensure the generation of novel accurate imaging tools which have sensitivity, specificity and resolution at improving levels. Accordingly, image denoising employs advanced algorithms to remove noise from graphics, which makes an impact on the quality of the images. The impact of the environment, channels related to transmission as well as related factors cause contamination by noise, which brings about loss of image information and distortion. The recovery of the meaningful information from noisy images to obtain high quality in images is challenging, as noted above. In view of a perspective based on mathematical foundation, image denoising is stated to be an inverse problem whose solution is not unique (Fan *et al.* 2019). Image noise reduction and feature preserving stand to be other challenges as image noise removal shows a relevant matter in different image analyses and computer vision-related matters where retaining the essential image features like the edges, corners and other sharp structures during smoothing and other related processes (Barbu 2014).

Fractional calculus is capable of attaining a satisfactory denoising effect, and the application of its theory provides important inputs in image denoising. Thus, fractional calculus can weaken high-frequency signal and preserving low-frequency signal in a nonlinear way, which means high-frequency noise can be removed while the information of low-frequency image itself can be retained (Wang *et al.* 2020). Concerning fractional calculus, in image denoising and image restoration, fractional derivatives have been employed in different studies (Bai and Feng 2007; Chen *et al.* 2013; Hilfer 2000; Herrmann 2011). (Abirami *et al.* 2021) considered the classical anisotropic diffusion model under the Caputo fractional derivative with a variable order of derivative function and achieved better performance for biomedical images like ultrasound, CT scans, x-rays and so forth. (Fang *et al.* 2020) presented a time-fractional model under the Caputo fractional derivative to remove additive noise and applied binary block partition to discretize their model. Another work (Janev *et al.* 2011) introduced a new fractional anisotropic diffusion equation for the aim of noise removal which contained spatial and time fractional derivatives. To construct a numerical scheme, the proposed partial differential equation (PDE) was used to preserve the edges (Janev *et al.* 2011).

One other paper introduces a new class of fractional-order anisotropic diffusion equations to remove noise. The authors employ the discrete Fourier transform for the implementation of the numerical algorithm. Besides outlining the various numerical results regarding the denoising of real images, the experiments of the study demonstrate the proposed fractional-order anisotropic diffusion equations capacity to yield good visual effects and better signal-to-noise ratio (Bai and Feng 2007). A novel class of fractional-order nonlinear anisotropic diffusion equations based image restoration model is established employing the p-Laplace norm of fractional-order gradient of an image intensity function is introduced in another paper where fractional-order gradient helps to better accommodate the images texture details. Thus, the proposed method removed noise and kept high-frequency edge of images in an efficient way nonlinearly (Yin *et al.* 2015). Another research provides a novel fast fractional order anisotropic diffusion algorithm to remove noise removal. The authors improve the algorithms efficiency by implementing the fast explicit format iteration algorithm with periodic change of time step size. Showing numerical results on denoising tasks and presenting of the experimental results corroborate that the algorithm can obtain satisfactory denoising results more quickly (Zhang *et al.* 2021).

Regarding multiplicative noise removal, a paper uses a maximum a posteriori (MAP) estimator and the authors derive a functional with a minimizer corresponding to the denoised image desired to be recovered (Aubert and Aujol 2008). Concerning image segmentation, hybrid methods are said to provide benefits compared to conventional means in inhomogeneous image segmentation. Accordingly, (Chen *et al.* 2019) presents a new hybrid method to integrate image gradient, local environment and global information into a specific framework. Image segmentation method based on PDE reveals strong vitality terms of image processing and computer vision. A new simple well-behaved definition of the fractional derivative which is named conformable fractional derivative is handled in (Othman and Shaw 2021), where a geometrical approach of fractional derivatives was introduced. For the purpose of obtaining the solution of fractional order differential equation (FDE) with the integer-order initial condition, certain new criteria regarding fractional derivatives are proposed in the study. Finally, reducing denoise in images multiplicatively (DIM) is modified in (Ibrahim 2020) with the aim of presenting a new technique based on a new fractional calculus to solve the problem termed as conformable fractional calculus (CFC) which provides benefits due it its formula involving a controller to be implemented for complex problems like DIM. Another study (Karaca and Baleanu 2022) aims to construct a robust and accurate model, which is based on fractional-order calculus (FOC) and Artificial Neural Network (ANN) integration, concerned with differentiability prediction and diagnosis of stroke and breast cancer, which pose complex problems considering the diseases highly complex neurological and biological properties.

Furthermore, (Khalil *et al.* 2014) propose a definition of a conformable fractional derivative and provide some properties of a fractional derivative. The conformable fractional- order derivative is an extended version of the classical fractional derivative, and it is very efficient in terms of obtaining the solution of the fractional-order PDEs. Consequently, the conformable fractional derivative encompasses diverse applications in science, engineering, and so forth. (Zhao and kang Luo 2017) proposed the physical interpretation and application of the general conformable fractional derivative. Many applications of fractional derivatives and fractional integrals are discussed by (Butera and Paola 2014; Contreras *et al.* 2018; Cresson 2010; Zhao and kang Luo 2017; Zhou *et al.* 2018), and the analytic solution of the time-fractional heat equation is also pointed out, which may be further resorted to in (Hammad and Khalil 2014a,b).

Considering these ends, the model presented by (Catté *et al.* 1992), concerned with edge detection and image selective smoothing by nonliear diffusion, has been extended and developed to remove the additive noise for the ultrasound image. The improved model in the scheme of our study as proposed includes the time-fractional derivative with smoothness diffusivity, and subsequently, the viscosity solution of the fractional diffusion model is proven through the scheme in question as compared to other relevant and parallel stuies existing in the literature, the first approach to remove noise and preserve edges by partial differential equations based anisotropic diffusion model is proposed by (Perona and Malik 1990). The improved (Perona and Malik 1990) model for image restoration and edge detection is introduced by (Catté *et al.* 1992). They have used the smoothing diffusivity i.e. $G_\sigma * u$, G_σ is the Gaussian smoothing kernel. The diffusion tensor based anisotropic diffusion model is proposed by (Weickert 1997). The additive Gaussian white noise based anisotropic diffusion model for image denoising and deblurring is given by (Welk *et al.* 2005) They have proposed the forward-backward diffusivity to discretize diffusion model.

The weighted and well balanced based anisotropic diffusion model is given by (Prasath and Vorotnikov 2014). The smooth Gaussian kernel based diffusion model for image restoration is proposed by (Kumar and Ahmad 2014; Kumar *et al.* 2016). Accordingly, a fractional derivative-based nonlinear anisotropic diffusion model for biomedical imaging has been presented to reduce additive Gaussian white noise in this study. The fractional order a appears in the time derivative and finds the results with different fractional order α. The performance of the ultrasound images is measured by the PSNR values. The experimental results of the fractional and classical diffusion models are computed by the finite-difference explicit scheme. The results demonstrate that the proposed model (5) has larger PSNR values corresponding to (3) at the different iteration numbers. This study has been conducted to attain better results for ultrasound images based on the novel and extended scheme based on the motivational aspect that reducing noise in images is an essential task in image processing.

The rest of the paper is structured in the following manner: Section 2 introduces the definition of Conformable Fractional Derivatives. Denoising Based Time Fractional Diffusion Algorithm is given in Section 3 and Theoretical Considerations for the Diffusion Model are introduced in Section 4. In Section 5, Discretized Scheme for the Anisotropic Diffusion and Fractional Anisotropic Diffusion Model is provided and depicted. Section 6 addresses Experimental Results of the Diffusion Model and Fractional Diffusion Model. Finally, Section 6 provides Conclusion, Discussions and Future Directions.

CONFORMABLE FRACTIONAL DERIVATIVES

The conformable fractional derivative which contains many applications and the conformable fractional derivative is implemented to anomalous diffusion by (Zhao and kang Luo 2017; Zhou *et al.* 2018). The fractional derivative function with the order α is as $h : (0, \infty) \to R$ and it is defined in the following way:

$$F_\alpha(h)(t) = F_\alpha h(t) = \lim_{\epsilon \to 0} \frac{h(t + \epsilon\, t^{1-\alpha}) - h(t)}{\epsilon},$$

provided the limit exists for all values $t > 0$ and $\alpha \in (0, 1)$.

The function h represented α- differentiable in $(0, a)$ for some $a > 0$ and also can be written as:

$$h^\alpha(0) = \lim_{t \to 0^+} h^\alpha(t). \tag{1}$$

If h is α- differentiable in the conformable sense at $t > 0$, then it must be differentiable in the classical sense at t and

$$F_\alpha h(t) = t^{1-\alpha} h'(t). \tag{2}$$

DENOISING BASED TIME FRACTIONAL DIFFUSION ALGORITHM

The nonlinear anisotropic diffusion models obtained remarkable success in the reduction of Gaussian noise, multiplicative noise etc., and this scheme depends on the parabolic partial differential equation introduced by (Perona and Malik 1990). By this scheme, edges can be preserved during the noise reduction and diffusion acts in an inhomogeneous way; it is maximum over the flat areas and has the lowest value over the edges. (Catté *et al.* 1992) introduced the Perona and Malik model improved for image restoration model and it can be denoted as below:

$$\frac{\partial u}{\partial t} = \nabla \cdot (\zeta(|\nabla G_\sigma * u|)\nabla u), \tag{3}$$

with homogeneous Neumann boundary conditions $\frac{\partial u}{\partial \vec{n}} = 0$ on the boundary of $\partial\Omega$ and Ω is a bounded domain of R^n, $\vec{n}$ the unit outer normal to Ω.

where G_σ is the Gaussian kernel and it is depends on scale parameter (Bai and Feng 2007), $*$ represents the notation for convolution i.e. $G_\sigma * u$. The solution of heat equation is equivalent to the convolution of the signal with Gaussian discussed by (Witkin 1983). Therefore, G_σ can be consider to be any smoothing kernel or low pass filter (Álvarez *et al.* 1992; Catté *et al.* 1992).

As indicated, the classical diffusion model is intended to be converted into (3) to the time-fractional diffusion model for biomedical imaging, which can be denoted as:

$$\frac{\partial^\alpha u}{\partial t^\alpha} = \nabla \cdot (\zeta(|\nabla G_\sigma * u|)\nabla u). \tag{4}$$

After applying the definition of the conformable fractional derivative as provided in section 2., equation (4) can be written as:

$$t^{1-\alpha} \frac{\partial u}{\partial t} = \nabla \cdot (\zeta(|\nabla G_\sigma * u|)\nabla u). \tag{5}$$

This is a PDE-based time-fractional diffusion model and α is the fractional order derivative and the diffusivity ζ, the diffusion threshold parameter K, s is the gradient of the image, and $\zeta(s)$ is a nonnegative function. The parameter K is used to the controlling the even enhancement of edges preserved. The Charbonnier diffusivity $\zeta(s) = \frac{1}{\sqrt{1+(|s|^2/K^2)}}$, related to the convex regularizer $\psi(s^2) = \sqrt{K^4 + K^2 s^2} - K^2$, can be resorted to in (Charbonnier *et al.* 1994; Weickert 1997) as used in the numerical experiments conducted in this study.

(Barbu *et al.* 2009) and (Strong 1997) have introduced the class of functions for the diffusion model and which can be defined as:

$$\zeta(x, |\nabla u|) = \delta \zeta_g(|\nabla u|). \tag{6}$$

The function ζ_g relies upon the magnitude of the gradient u and it can be similar to $\zeta(s)$ and δ is the adaptive parameter. We choose the values of $\delta(x) = 1$, $\zeta_g = \zeta(s)$, $G_\sigma * u$ as u. Then the fractional diffusion model (4) it can be presented in another form as follows:

$$\frac{\partial^\alpha u}{\partial t^\alpha} = \nabla \cdot (\zeta(x, |\nabla u|)\nabla u). \tag{7}$$

Motivated by (Álvarez *et al.* 1992; Prasath and Vorotnikov 2014) and (Giga *et al.* 2022), we want to show the theoretical considerations and viscosity solution of the fractional diffusion model in the next section.

THEORETICAL CONSIDERATIONS FOR THE FRACTIONAL DIFFUSION MODEL

This section provides the viscosity solution and some theoretical considerations for the diffusion model (7):

$$\frac{\partial^\alpha u}{\partial t^\alpha} = \nabla \cdot (\zeta(x, |\nabla u|)\nabla u), \tag{8}$$

Let x and q be two auxiliary functions that are defined from $\mathbb{R}^n$. A vector χ, symmetric matrix c then, the following equations are to be noted

$$c_{ij}(x,q) = \zeta(x,|q|)\delta_{ij} + \zeta_y(x,|q|)\frac{q_i q_j}{|q|}, \tag{9}$$

$$\chi_i(x,q) = \frac{\partial \zeta(x,|q|)}{\partial x_i}. \tag{10}$$

In this part, δ_{ij} is the Kronecker's delta and ζ_y is the partial derivative w.r.to y of the function $\zeta(x,y)$. (Alvarez and Esclarin 1997) have proposed the spatially periodic boundary conditions; thus may we assume that the orthogonal basis b_i in $\mathbb{R}^n$ is defined as

$$u(.,x+b_i) = u(.,x), \quad x \in \mathbb{R}^n, \;\; i = 1,2,....n. \tag{11}$$

The functions c and χ are bounded continuously differentiable in x, periodic and x-derivatives are uniformly bounded w.r.t. q. The function u_0 Lipschitz and satisfy equation (11). ζ and (c and χ) satisfy periodicity restriction w.r.to x but not to y or q.

$$c_{ij}(x,q)\xi_i\xi_j \geq K\left[\text{mod}\left(\frac{\partial c(x,q)}{\partial x_k}\right)\right]_{ij}\xi_i\xi_j, \quad k = 1,.......n, \; \xi, x, q \in \mathbb{R}^n. \tag{12}$$

The generic positive constant number K for different values in different lines.

The viscosity subsolution and super solution is known as the viscosity solution for equation (8), if $\Psi \in K^2([0,T] \times \mathbb{R}^n)$ is any function and $(x_0,t_0) \in (0,T] \times \mathbb{R}^n$ is any point then $u - \phi$ attains local maximum/minimum (Evans and Spruck 1991) and the equivalence of the viscosity solution (Giga *et al.* 2022) as follows:

$$\frac{\partial \Psi^\alpha(x_0,t_0)}{\partial t^\alpha} - \nabla \cdot (\zeta(x_0, |\nabla \Psi(x_0,t_0)|)\nabla \Psi(x_0,t_0)) \leq 0/\geq 0 \tag{13}$$

Lemma. The quadratic matrices of order $n \times n$ are P and Q. Let Q is symmetric matrix then a constant number $N \geq 0$ can be defined as

$$NP_{ij}\xi_i\xi_j \geq \text{mod }(Q)_{ij}\xi_i\xi_j, \quad \forall\, \xi \in \mathbb{R}^n. \tag{14}$$

For every matrix U is not necessarily symmetric of order $n \times n$ has

$$Tr^2(QU^\top) \leq N||Q||Tr(UPU^\top). \tag{15}$$

Here the norm operator of a matrix is denoted by $||.||$ and Q is the matrix whose pixel values are positive.

Proof. From equations (14) and (15) are invariant w.r.to to orthogonal changes of bases. We can therefore assume that Q has already been diagonalized by an axial transform without losing generality. Then

$$\begin{aligned} Tr^2(QU^\top) &= (Q_{ii}U_{ii})^2 \leq ||Q||Q_{ii}U_{ii}^2 \\ &= ||Q||(\text{mod}(Q)_{ii}U_{ii}^2 \leq ||Q||(\text{mod}(Q)_{ii}U_{ki}U_{kj} \\ &= ||Q||(\text{mod}(Q)_{ij}U_{ki}U_{kj} \leq N||Q||P_{ij}U_{ki}U_{kj} = N||Q||Tr(UPU^\top). \end{aligned}$$

Theorem. A function $u \in K([0,T] \times \mathbb{R}^n) \cap L^\infty(0,T,W^{1,\infty}(\mathbb{R}^n))$ is a viscosity solution (8) for any $T \in [0,\infty)$, if $v \in K(\mathbb{R}^n \times [0,T))$ is a viscosity solution of (8) then a periodic function u_0 is Lipschitz continuous on $\mathbb{R}^n$ is replaced by Lipschitz continuous function v_0 for any $T \in [0,\infty)$, then there exist a positive number K, which depends on T, u_0 and v_0 as below:

$$\sup_{0\leq t\leq T} ||u(x,t) - v(x,t)||_{L^\infty(\mathbb{R}^n)} \leq K||u_0 - v_0||_{L^\infty(\mathbb{R}^n)}. \tag{16}$$

Furthermore, $\inf_{\mathbb{R}^n} u_0 \leq u(x,t) \leq \sup_{\mathbb{R}^n} u_0$.

The diffusion model (8) which contains the viscosity sub/super solution. i.e. a unique viscosity solution u.

Proof. The viscosity solution u of (8) on $\mathbb{R}^n \times \mathbb{R}^+$ satisfy the inequality:

$$\inf_{\mathbb{R}^n} u_0 \leq u(x,t) \leq \sup_{\mathbb{R}^n} u_0, \;\; \text{on} \;\; \mathbb{R}^n \times \mathbb{R}_+. \tag{17}$$

Let $\Psi(x,t) = \delta t$ at the point (x_0,t_0), $t_0 > 0$, of the global maximum of $u(x,t) - \delta t$, the equation (13) gives $\delta + \lambda(u(t_0,x_0) - u_0(x_0)) \leq 0$, when $u(x_0,t_0) < u_0(x_0)$, it is contradiction because $u(x_0,t_0) - \delta t_0 \geq u_0(x_0)$, then $u(x,t) - \delta t$ achieves a global maximum at $t = 0$, and let $\delta \to 0^+$ and (x_0,t_0) is the global maximum point thus we get (17).

The formal a priori estimate for $\sup_{\mathbb{R}^n}|\nabla u|$ is established. It should be noted that (8) is identical to such that:

$$\frac{\partial^\alpha u}{\partial t^\alpha} = [c_{ij}(x,\nabla u)u_{x_i x_j} + \chi_i(x,\nabla u)u_{x_i}]. \tag{18}$$

The equation (18) differentiate in relation to each x_k, $k = 1,...,n$, and through the multiplication by $2u_{x_k}$ and taking a summation with respect to k, we obtain

$$\begin{aligned} \beta(|\nabla u|^2) := {} & \frac{\partial^\alpha |\nabla u|^2}{\partial t^\alpha} - c_{ij}(x,\nabla u)\frac{\partial^2}{\partial x_i \partial x_j}|\nabla u|^2 - \\ & \frac{\partial c_{ij}(x,\nabla u)}{\partial p_l}u_{x_i x_j}\frac{\partial}{\partial x_l}|\nabla u|^2 - \chi_i(x,\nabla u)\frac{\partial}{\partial_i}|\nabla u|^2 - \\ & \frac{\partial \chi_i(x,\nabla u)}{\partial p_l}u_{x_i}\frac{\partial}{\partial x_l}|\nabla u|^2 \\ & = -2c_{ij}(x,\nabla u)u_{x_k x_i}u_{x_k x_j} + 2\frac{\partial c_{ij}(x,\nabla u)}{\partial x_k}u_{x_i x_j}u_{x_k} \\ & + 2\frac{\partial \chi_{ij}(x,\nabla u)}{\partial x_k}u_{x_i}u_{x_k}. \end{aligned} \tag{19}$$

The option to eliminate the second term's undesirable influence from the right side of (19) and using Cauchy's inequality for the second term and Lemma 3.1, we obtain

$$\begin{aligned} \left|2\frac{\partial c_{ij}(x,\nabla u)}{\partial x_k}u_{x_i x_j}u_{x_k}\right| &\leq K|u_{x_k}|\sqrt{c_{ij}(x,\nabla u)u_{x_k x_i}u_{x_k x_j}} \\ &\leq c_{ij}(x,\nabla)u_{x_k x_i}u_{x_k x_j} + K|\nabla u|^2. \end{aligned} \tag{20}$$

From the equation (19), the sum of the terms does not exceed $K(1+|\nabla u|^2)$. Hence,

$$\beta(|\nabla u|^2) \leq K(1+|\nabla u|^2), \tag{21}$$

$$\beta(e^{-Kt}(1+|\nabla u|^2)) \leq 0. \tag{22}$$

Using the definition of the weak maximum principle, the operator β can be yield

$$|\nabla u|^2 \leq K. \tag{23}$$

The uniform Hölder estimate by equation (17) and (23) (Alvarez and Esclarin 1997). we can denote the following:

$$|u(x,t) - u(x,r)|^2 \leq K|t-r|. \tag{24}$$

The solution of these equations (17), (23) and (24) are uniformly bounded and equicontinuous on $\mathbb{R}^n \times [0, T]$ and also satisfy the stability results (Crandall *et al.* 1992). The uniqueness solutions exist by the stability estimate of the equation (16) and proof of a similar bound and the matrix τ, the following work can be referred to (Shi and Chang 2006) by replaced by

$$\tau = \begin{pmatrix} M_1 & \sqrt{M_1}\sqrt{M_2} \\ \sqrt{M_1}\sqrt{M_2} & M_2 \end{pmatrix}, \tag{25}$$

where

$$M_1 = d\left(x_0, \frac{|x_0-y_0|^2(x_0-y_0)}{\delta}\right),\ M_2 = d\left(y_0, \frac{|x_0-y_0|^2(x_0-y_0)}{\delta}\right).$$

DISCRETIZED SCHEME FOR THE ANISOTROPIC DIFFUSION AND FRACTIONAL ANISOTROPIC DIFFUSION MODEL

The discretized scheme for both anisotropic diffusion and fractional anisotropic diffusion model is discussed herein. Let $x_i = i\Delta x$, $y_j = j\Delta x$, i, j=1,2,3.......N, $N\Delta x = 1$, (Δx is spatial step size) and $t_n = n\Delta t$, $\;n \geq 1$ (Δt is the time step size).

It is possible to denote the explicit scheme of (5) as follows:

$$u^t_{ij} = t^{\alpha-1}\frac{1}{2\Delta x}\left[(\zeta^n_{i+1,j}+\zeta^n_{i,j})(u^n_{i+1,j}-u_{i,j}) - (\zeta^n_{i,j}+\zeta^n_{i-1,j})(u^n_{i,j}-u^n_{i-1,j})\right]$$

$$+t^{\alpha-1}\frac{1}{2\Delta x}\left[(\zeta^n_{i,j+1}+\zeta^n_{i,j})(u^n_{i,j+1}-u_{i,j}) - (\zeta^n_{i,j}+\zeta^n_{i,j-1})(u^n_{i,j}-u^n_{i,j-1})\right]).$$

It is similar to the discrete scheme for the diffusion model (3) if $\alpha = 1$.

The diffusivity $\zeta(|\nabla u|^2)$ is discretized by,

$$\zeta^n_{ij} = \psi'\left(\left(\frac{u^n_{i+1,j}-u^n_{i-1,j}}{\Delta x}\right)^2 + \left(\frac{u^n_{i,j+1}-u^n_{i,j-1}}{\Delta x}\right)^2\right),$$

The explicit method is stable and convergent for $\Delta t/\Delta x^2 < 0.5$, see (Lapidus and Pinder 1983). The numerical explicit scheme (5) is stable and consistent with the diffusion based fractional model. It is then used in our numerical experiments which are given in the next section.

EXPERIMENTAL RESULTS OF THE DIFFUSION MODEL AND FRACTIONAL DIFFUSION MODEL

In this section, we want to give experimental results of the diffusion model and proposed fractional diffusion model for original ultrasound images are taken (Al-Dhabyani *et al.* 2020). The original images size 256×256 contain the pixel value [0, 255]. To perform the experiments, we reduce the pixel value of all images in between [0, 1]. Speckle noise can be added by the function imnoise(u, 'speckle', σ) in Matlab [MATLAB, 2022 version 9.12.0 (R2022a). The Math-Works Inc., Natick, Massachusetts]. In our all experiment, we have taken the parameters $\Delta t/\Delta x^2 = 0.45$, diffusivity parameter $K = 5$, time parameter $t = 0.02$ and $\lambda = 0.85$, see reference (Hammad and Khalil 2014b; Chan *et al.* 1999; Chang and Chern 2003).

The experimental results for different fractional orders significantly reduce the iteration step and better PSNR value provided herein. The fractional-order α proves to be very important in the experiment. This is because a small fractional-order α will get more clarity denoising the image at a smaller number of iterations. We check the clarity of the denoising image by the PSNR value. The larger PSNR value of the images has a satisfactory level of result, while the fractional model provides fast process images when image denoising and edge-preserving are conducted together. To check the quality of the denoised image, the following denotation is to be referred to:

$$\text{PSNR} = 10\log_{10}\left(\frac{S^2}{\frac{1}{MN}\sum^n_{i,j}(u_1(i,j)-u(i,j))^2}\right). \tag{26}$$

Here $u_1(i,j)$ and $u_(i,j)$ are the restored and original image respectively, S is the maximum pixel value of the image and MN is the order of the matrix.

Ultrasound image and breast cancer benign ultrasound images are provided in Figure 1 (a) and (b). In addition, Figure 2 provides the speckle noisy image (σ = 0.1) and related denoised images, whereas Figure 3 presents the speckle noisy image (σ = 0.3) and related denoised images. Figure 4 shows the speckle noisy image (σ = 0.5) and related denoised images, while Figure 5 depicts the speckle noisy image (σ= 0.06) and related denoised images. Figure 6 provides the speckle noisy image (σ = 0.08) and related denoised images, whereas Figure 7 presents the speckle noisy image (σ= 0.10) and related denoised images.

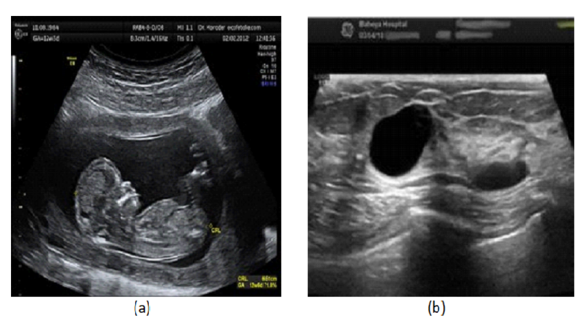

Figure 1 (a) Ultrasound image and (b) breast cancer benign ultrasound image.

The experimental results provided in terms of PSNR values with different levels of speckle noise ($\sigma = 0.1, 0.3, 0.5$) by using models (3) and (5) can be seen in Table 1.

The experimental results provided in terms of PSNR values with different levels of speckle noise ($\sigma = 0.06, 0.08, 0.10$) by using models (3) and (5) can be seen in Table 2.

Table 1 The experimental results in terms of PSNR values with different levels of speckle noise (σ = 0.1, 0.3, 0.5) by using models (3) and (5).

Images	PSNR for the noisy images	PSNR for the denoised images by model (3)	PSNR for the denoised images by model (5)			
			$\alpha = 0.7$	$\alpha = 0.5$	$\alpha = 0.3$	$\alpha = 0.1$
Figure 2(a-f)	22.19	22.76	23.12	24.22	25.25	25.66
Figure 3(a-f)	17.69	18.20	18.57	19.36	21.03	22.94
Figure 4(a-f)	15.87	16.33	16.64	17.47	19.02	21.17
No. of iterations		100	50	50	50	50

Table 2 The experimental results in terms of PSNR values with different levels of speckle noise (σ = 0.06, 0.08, 0.10) by using models (3) and (5).

Images	PSNR for the noisy images	PSNR for the denoised images by model (3)	PSNR for the denoised images by model (5)			
			$\alpha = 0.7$	$\alpha = 0.5$	$\alpha = 0.3$	$\alpha = 0.1$
Figure 5(a-f)	21.80	22.07	22.26	22.43	23.32	24.10
Figure 6(a-f)	20.62	21.18	21.35	21.50	22.75	23.88
Figure 7(a-f)	19.66	20.29	20.66	20.85	22.24	23.52
No. of iterations		300	100	50	50	50

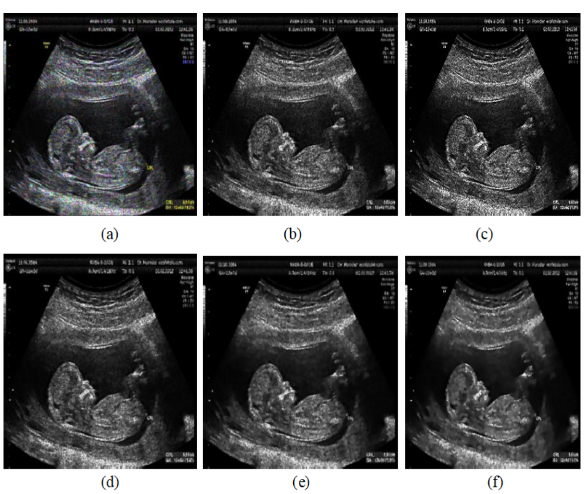

Figure 2 (a) Speckle noisy image with ($\sigma = 0.1$); (b) Denoised image by (3); (c-f) Denoised images by (5) at $\alpha = 0.7, 0.5, 0.3$ and 0.1, respectively.

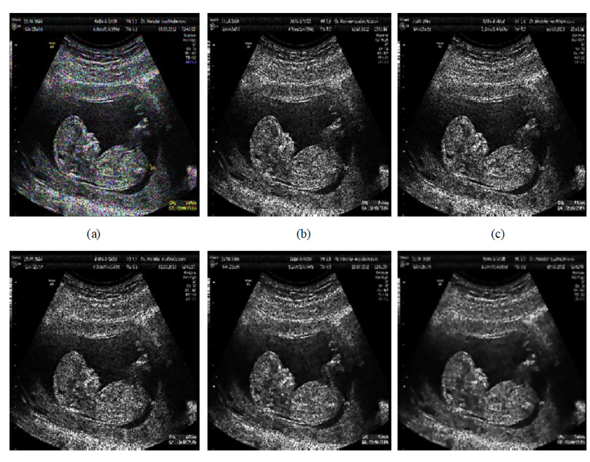

Figure 3 (a) Speckle noisy image with ($\sigma = 0.3$); (b) Denoised image by (3); (c-f) Denoised images by (5) at $\alpha = 0.7, 0.5, 0.3$ and 0.1, respectively.

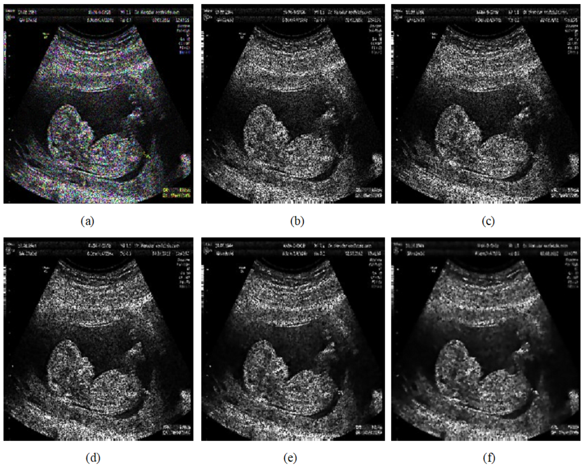

Figure 4 (a) Speckle noisy image with ($\sigma = 0.5$); (b) Denoised image by (3); (c-f) Denoised images by (5) at $\alpha = 0.7, 0.5, 0.3$ and 0.1 in the related order.

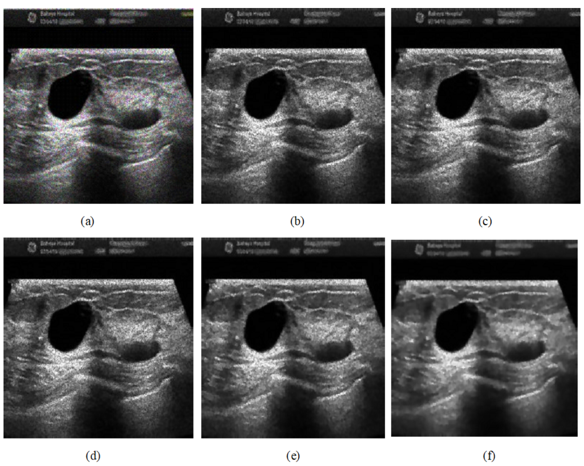

Figure 5 (a) Speckle noisy image with ($\sigma = 0.06$); (b) Denoised image by (3); (c-f) Denoised images by (5) at $\alpha = 0.7, 0.5, 0.3$ and 0.1, respectively.

CONCLUSION, DISCUSSIONS AND FUTURE DIRECTIONS

Reducing noise in images is a critical task for accuracy and precision in image processing, and it is possible that noises can emerge with images through achievement pertaining to diffusion. Accordingly, a fractional order derivative-based diffusion model for biomedical imaging has been presented to reduce additive speckle noise. The medical images (ultrasound image, X-rays, CT scans, MRIs, etc.) may lose significant features and become degraded due to the emergence of noise. Detecting the additive noise in the images and finding the applicable solution in a timely manner becomes particularly essential, which is a detecting the additive noise in the images and finding the solution to such matters becomes a challenge to be tacked effectively for researchers, clinicians, pharmaceutical authorities and related practitioners.

The aim of this study has been to prove the viscosity solution of the diffusion model with the proposed model providing to be efficient in reducing noise by preserving the essential image features like edges, corners and other sharp structures for ultrasound images in comparison to the classical anisotropic diffusion model. Consequently, this paper has presented a conformable fractional

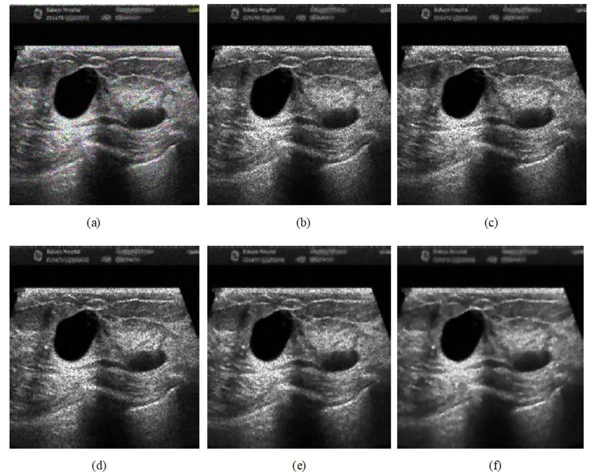

Figure 6 (a) Speckle noisy image with ($\sigma = 0.08$); (b) Denoised image by (3); (c-f) Denoised images by (5) at $\alpha = 0.7, 0.5, 0.3$ and 0.1, respectively.

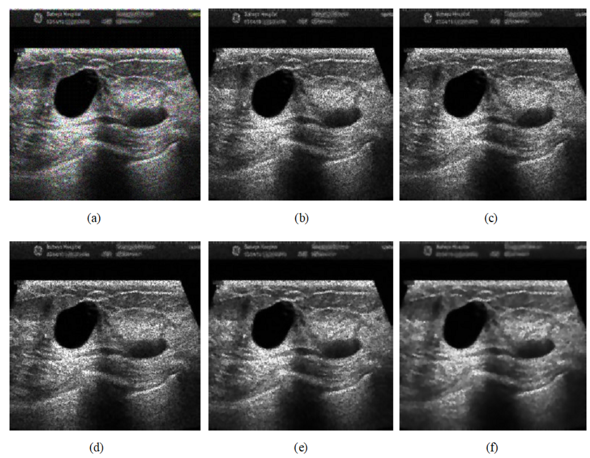

Figure 7 (a) Speckle noisy image with ($\sigma = 0.10$); (b) Denoised image by (3); (c-f) Denoised images by (5) at $\alpha = 0.7, 0.5, 0.3$ and 0.1, respectively.

derivative-based anisotropic diffusion model for removing speckle noise in ultrasound images to attain the optimal outcomes. The finite difference method has been used to discretize the fractional diffusion model and classical diffusion models. The peak signal-to-noise ratio (PSNR) has also been used for the quality of the smooth images. The proposed mathematical model in this study is a generalization of the classical diffusion model. The fractional order α appears in the time derivative and finds the results with different fractional order a. The performance of the ultrasound images is measured by the PSNR values.

The comparative experimental results of the fractional and classical diffusion models as presented herein are computed by the finite difference explicit scheme. Thus, the results demonstrate that the proposed mathematical model (5) has larger PSNR values corresponding to (3) at the different iteration number. We may, therefore, draw the conclusion that the proposed model obtained yield better results for ultrasound images based on the novel and extended scheme. Another relevant novel contribution has been that the improved mathematical model in the scheme of our study based on the experimental results, as has been proposed, includes the time-fractional derivative with smoothness diffusivity, and subsequently, the viscosity solution of the fractional diffusion model has been proven through the scheme under consideration. In future endeavors, the applicability of various fractional derivatives on these mathematical diffusion-related and other equivalent schemes can be compared and put forth to serve biomedical imaging like X-rays, CT scans, MRIs, etc., bioengineering and other related medical, clinical and image-signal related applied as well as computational processes.

Availability of data and material

Not applicable.

Conflicts of interest

The authors declare that there is no conflict of interest regarding the publication of this paper.

Ethical standard

The authors have no relevant financial or non-financial interests to disclose.

LITERATURE CITED

Abirami, A., P. Prakash, and Y.-K. Ma, 2021 Variable-Order Fractional Diffusion Model-Based Medical Image Denoising. Mathematical Problems in Engineering **2021**: 1–10.

Al-Dhabyani, W., M. Gomaa, H. Khaled, and A. Fahmy, 2020 Dataset of breast ultrasound images. Data in Brief **28**: 104863.

Alvarez, L. and J. Esclarin, 1997 Image quantization using reaction-diffusion equations. SIAM Journal on Applied Mathematics **57**: 153–175.

Álvarez, L., P.-L. Lions, and J.-M. Morel, 1992 Image selective smoothing and edge detection by nonlinear diffusion. ii. SIAM Journal on Numerical Analysis **29**: 845–866.

Aubert, G. and J.-F. Aujol, 2008 A variational approach to removing multiplicative noise. SIAM Journal on Applied Mathematics **68**: 925–946.

Bai, J. and X.-C. Feng, 2007 Fractional-order anisotropic diffusion for image denoising. IEEE Transactions on Image Processing **16**: 2492–2502.

Barbu, T., 2014 Robust anisotropic diffusion scheme for image noise removal. Procedia Computer Science **35**: 522–530, Knowledge-Based and Intelligent Information and Engineering Systems 18th Annual Conference, KES-2014 Gdynia, Poland, September 2014 Proceedings.

Barbu, T., V. Barbu, V. Biga, and D. Coca, 2009 A pde variational approach to image denoising and restoration. Nonlinear Analysis: Real World Applications **10**: 1351–1361.

Butera, S. and M. D. Paola, 2014 A physically based connection between fractional calculus and fractal geometry. Annals of Physics **350**: 146–158.

Catté, F., P. Lions, J. Morel, and T. Coll, 1992 Image selective smoothing and edge detection by nonlinear diffusion*. SIAM J. Numer. Anal. **29**: 182–193.

Chan, T. F., G. H. Golub, and P. Mulet, 1999 A nonlinear primal-dual method for total variation-based image restoration. SIAM J. Sci. Comput. **20**: 1964–1977.

Chang, Q. and I.-L. Chern, 2003 Acceleration methods for total variation-based image denoising. SIAM Journal on Scientific Computing **25**: 982–994.

Charbonnier, P., L. Blanc-Féraud, G. Aubert, and M. Barlaud, 1994 Two deterministic half-quadratic regularization algorithms for computed imaging. Proceedings of 1st International Conference on Image Processing **2**: 168–172 vol.2.

Chen, B., S. Huang, Z. Liang, W. Chen, and B. Pan, 2019 A fractional order derivative based active contour model for inhomogeneous image segmentation. Applied Mathematical Modelling **65**: 120–136.

Chen, D., S. Sun, C. Zhang, Y. Chen, and D. Xue, 2013 Fractional-order TV-L^2 model for image denoising. Central European Journal of Physics **11**: 1414–1422.

Contreras, A. O., J. Rosales, L. M. Jimenez, and J. M. Cruz-Duarte, 2018 Analysis of projectile motion in view of conformable derivative. Open Physics **16**: 581–587.

Crandall, M. G., H. Ishii, and P.-L. Lions, 1992 Users guide to viscosity solutions of second order partial differential equations. Bulletin of the American Mathematical Society **27**: 1–67.

Cresson, J., 2010 Inverse problem of fractional calculus of variations for partial differential equations. Communications in Nonlinear Science and Numerical Simulation **15**: 987–996.

Evans, L. C. and J. Spruck, 1991 Motion of level sets by mean curvature. I. Journal of Differential Geometry **33**: 635–681.

Fan, L., F. Zhang, H. Fan, and C. Zhang, 2019 Brief review of image denoising techniques. Vis. Comput. Ind. Biomed. Art **2**.

Fang, Z.-W., H.-W. Sun, and H. Wang, 2020 A fast method for variable-order caputo fractional derivative with applications to time-fractional diffusion equations. Computers and Mathematics with Applications **80**: 1443–1458.

Giga, Y., H. Mitake, and S. Sato, 2022 On the equivalence of viscosity solutions and distributional solutions for the time-fractional diffusion equation. Journal of Differential Equations **316**: 364–386.

Gilboa, G., N. Sochen, and Y. Zeevi, 2006 Variational denoising of partly textured images by spatially varying constraints. IEEE Transactions on Image Processing **15**: 2281–2289.

Hammad, I. A. and R. Khalil, 2014a Fractional fourier series with applications. American Journal of Computational and Applied Mathematics **4**: 187–191.

Hammad, M. A. and R. Khalil, 2014b Conformable fractional heat differential equation. International journal of pure and applied mathematics **94**: 215–221.

Herrmann, R., 2011 *Fractional Calculus: An Introduction for Physicists*. World Scientific.

Hilfer, R., 2000 *Applications of Fractional Calculus in Physics*. World Scientific.

Ibrahim, W. R., 2020 A new image denoising model utilizing the conformable fractional calculus for multiplicative noise. SN Applied Sciences **2**: 120–136.

Janev, M., S. Pilipoviaea, T. Atanackoviaea, R. Obradoviaea, and N. Raleviaea, 2011 Fully fractional anisotropic diffusion for image denoising. Mathematical and Computer Modelling **54**: 729–741.

Karaca, Y. and D. Baleanu, 2022 Chapter 9 - computational fractional-order calculus and classical calculus ai for comparative differentiability prediction analyses of complex-systems-grounded paradigm. In *Multi-Chaos, Fractal and Multi-Fractional Artificial Intelligence of Different Complex Systems*, edited by Y. Karaca, D. Baleanu, Y.-D. Zhang, O. Gervasi, and M. Moonis, pp. 149–168, Academic Press.

Khalil, R., M. Al Horani, A. Yousef, and M. Sababheh, 2014 A new definition of fractional derivative. Journal of Computational and Applied Mathematics **264**: 65–70.

Kumar, S. and M. Ahmad, 2014 A time dependent model for image denoising. Journal of Signal and Information Processing **6**: 28–

38.
Kumar, S., M. Sarfaraz, and M. Ahmad, 2016 An efficient pde-based nonlinear anisotropic diffusion model for image denoising. Neural, Parallel and Scientific Computations **24**: 305–315.
Lapidus, L. and G. F. Pinder, 1983 Numerical solution of partial differential equations in science and engineering. SIAM Review **25**: 581–582.
Mazloum, B. and H. Siahkal-Mahalle, 2022 A time-splitting local meshfree approach for time-fractional anisotropic diffusion equation: application in image denoising. Adv Cont Discr Mod **56**.
Othman, M. I. A. and S. Shaw, 2021 On the concept of a conformable fractional differential equation. Journal of Engineering and Thermal Sciences **1**: 17–29.
Perona, P. and J. Malik, 1990 Scale-space and edge detection using anisotropic diffusion. IEEE Trans. Pattern Anal. Mach. Intell. **12**: 629–639.
Prasath, V. B. S. and D. Vorotnikov, 2014 Weighted and well-balanced anisotropic diffusion scheme for image denoising and restoration. Nonlinear Analysis-real World Applications **17**: 33–46.
Shi, Y. and Q. Chang, 2006 New time dependent model for image restoration. Applied Mathematics and Computation **179**: 121–134.
Strong, D., 1997 *Adaptive total variation minimizing image restoration*.
Wang, Q., J. Ma, S. Yu, and L. Tan, 2020 Noise detection and image denoising based on fractional calculus. Chaos, Solitons and Fractals **131**: 109463.
Weickert, J., 1997 A review of nonlinear diffusion filtering. In *Scale-Space Theory in Computer Vision*, edited by B. ter Haar Romeny, L. Florack, J. Koenderink, and M. Viergever, pp. 1–28, Berlin, Heidelberg, Springer Berlin Heidelberg.
Welk, M., D. Theis, T. Brox, and J. Weickert, 2005 Pde-based deconvolution with forward-backward diffusivities and diffusion tensors. In *Scale Space and PDE Methods in Computer Vision*, edited by R. Kimmel, N. A. Sochen, and J. Weickert, pp. 585–597, Berlin, Heidelberg, Springer Berlin Heidelberg.
Witkin, A. P., 1983 Scale-space filtering. In *International Joint Conference on Artificial Intelligence*.
Yin, X., S. Zhou, and M. A. Siddique, 2015 Fractional nonlinear anisotropic diffusion with p-laplace variation method for image restoration. Multimedia Tools and Applications **75**: 4505 – 4526.
Zhang, Z., Q. Liu, and T. Gao, 2021 A fast explicit diffusion algorithm of fractional order anisotropic diffusion for image denoising.
Zhao, D. and M. kang Luo, 2017 General conformable fractional derivative and its physical interpretation. Calcolo **54**: 903–917.
Zhou, H., S. Yang, and S. Zhang, 2018 Conformable derivative approach to anomalous diffusion. Physica A: Statistical Mechanics and its Applications **491**: 1001–1013.

How to cite this article: Chauhan, A., Kumar, S., and Karaca, Y. A New Fractional-order Derivative-based Nonlinear Anisotropic Diffusion Model for Biomedical Imaging. *Chaos Theory and Applications*, 5(3), 198-206, 2023.